J Mater Sci

Chemical routes to materials

Ethanol–water-assisted room temperature synthesis of $CsPbBr_3/SiO_2$ nanocomposites with high stability in ethanol

Wen Li[1], Fengjun Chun[1], Xiaoqiang Fan[1], Wen Deng[1], Meilin Xie[1], Chao Luo[1], Shiyu Yang[1], Hanan Osman[1], Chuanqi Liu[2], and Weiqing Yang[1,*]

[1] *Key Laboratory of Advanced Technologies of Materials (Ministry of Education), School of Materials Science and Engineering, Southwest Jiaotong University, Chengdu 610031, China*

[2] *College of Optoelectronic Technology, Chengdu University of Information Technology, Chengdu 610225, China*

Received: 18 July 2018
Accepted: 1 November 2018

ABSTRACT

All-inorganic halide perovskites have attracted great attention by virtue of the merits of bright emission, tunable wavelength and narrow-band emission. Despite the excellent optical features, all-inorganic halide perovskite materials have suffered from intrinsic instability, which has limited their applications in various optoelectronic devices. To mitigate the intractable issue, we demonstrated the $CsPbBr_3$ nanoparticles decorated with smaller SiO_2 nanocrystals to passivate the surface defects; SiO_2 nanoparticles were applied as a barrier layer to maintain the optical property and enhance environmental stability. A facile in situ method was proposed to prepare $CsPbBr_3/SiO_2$ nanocomposites, in which an environmental ethanol/water solvent system was needed with the addition of tetraethyl orthosilicate (TEOS) as a silicon precursor. The obtained $CsPbBr_3/SiO_2$ nanocomposites have better optical characteristic and stability than bare $CsPbBr_3$ nanoparticles. Even 70% photoluminescence intensity of as-prepared $CsPbBr_3/SiO_2$ nanocomposites can be maintained after 168 h storage in ethanol. This newly developed synthesis will open up a new route for the fabrication of optoelectronic devices in an environmentally friendly way, and the as-obtained perovskite materials with improved stability will make them great potential for multifunctional optoelectronic devices.

Introduction

Among the various semiconductor nanocrystals, $CsPbX_3$ (X = I, Br, Cl), all-inorganic perovskite materials are particularly attractive owing to their superior optical and electronic properties, such as high photoluminescence quantum yield (PLQY), high color tunability, narrow emission line width and low trap state density [1–3]. In the past few years, researchers have witnessed the impressive advances of all-inorganic

Address correspondence to E-mail: wqyang@swjtu.edu.cn

https://doi.org/10.1007/s10853-018-3104-8

Published online: 07 November 2018

perovskite, which render them highly appealing in solar cells [4, 5], light emitting diodes (LED) [6, 7], photodetectors [8, 9] and lasers [10, 11]. However, due to their predominantly soft ionic crystal structure, intrinsic chemical instability remains the major issue, especially triggered by polar solvents, oxygen, thermal treatment and continuous light illumination [12–14]. Therefore, it is necessary to seek for a simple and convenient means to alleviate the instability issue.

In order to achieve relatively high stability of perovskite, many researchers have developed new strategies to address this critical issue and maintain the excellent luminescence characteristics, such as surface capping and embedding perovskite into organic or inorganic matrix. Recently, Liu et al. [15] demonstrated that cubic-stable $CsPbI_3$ quantum dots were achieved by introducing an organolead precursor (trioctylphosphine–PbI_2) with quantum efficiency up to 100%, negligible electron or hole-trapping pathways of the prepared $CsPbI_3$ quantum dots were detected. To avoid neutralization of conventional carboxylate and ammonium capping ligands, Krieg et al. and Pan et al. [16, 17] utilized the zwitterionic and bidentate capping ligands to improve the chemical durability of colloidal $CsPbX_3$ nanocrystals, respectively. However, the surface ligands are liable to desorb when the nanocrystals undergo the purification procedure, resulting in loss of colloidal chemical durability. Other works suggested that barrier materials are effective to protect perovskite nanocrystals from moisture, oxidation and other chemical attacks. Xin et al. [18] reported a green growth of $CsPbBr_3$/polymer composites without organic solvent; diverse perovskite–polymer composites were prepared and showed highly excellent resistance against water. Hou et al. [19] developed core–shell colloidal nanocrystals with a nanosized copolymer shell, polystyrene-block-poly-2-vinylpyridine (PS-b-P2VP), which passivated surfaces of $CsPbBr_3$ nanocrystals effectively. But the organic matrix materials always have lower photooxidation and thermal stability, which is a limiting factor for broad applications. Conversely, most inorganic matrix materials have better mechanical strength and thermal stability, such as silica oxide (SiO_2), titanium oxide (TiO_2) and alumina (Al_2O_3) [20–22]. In particular, SiO_2 has a high level of barrier property against moisture and temperature. The embedding of perovskite nanocrystals in mesoporous silica matrices has been reported by many research groups, and Wang et al. also proved that mesoporous silica can address the anion exchange effect and increase stability of perovskite materials [23–27]. However, mesoporous silica with intrinsic hydrophilicity and high specific surface area cannot completely block the hazard of moisture and oxygen, and the preparation of mesoporous silica is a complex and high cost process. The above situations prompt us to focus on solid SiO_2. Sun et al. [28] selected (3-aminopropyl)triethoxysilane (APTES) as the precursor for a silica matrix, and APTES was hydrolyzed to SiO_2 by capturing trace water vapor; then, quantum dot/silica composites were formed by a water-free synthesis system to increase the chemical stability. Li et al. [29] reported an amination-mediated nucleation and growth process to synthesize highly stable perovskite quantum dot anchored on SiO_2 surface, in which SiO_2 spheres were prepared separately. Hu et al. [30] combined a water-triggered transformation process and a solgel method to prepare monodisperse $CsPbX_3/SiO_2$ and $CsPbBr_3/Ta_2O_5$ Janus nanoparticles with improved stability; trace water was not only contributed to the stripping of CsBr from Cs_4PbBr_6 but also the formation of SiO_2. Due to their strong ionic nature, $CsPbX_3$ nanocrystals are extremely sensitive to water and ethanol; a small amount of water was added in most reported works. But conventional Stöber and reverse microemulsion methods always need water and ethanol as the media, and this limitation brings obstacles to modify the stability of perovskites with SiO_2.

In this paper, we developed an ethanol–water-assisted room temperature synthesis, in which high-quality $CsPbBr_3/SiO_2$ nanocomposites can be obtained. The as-prepared $CsPbBr_3/SiO_2$ nanocomposites showed improved chemical stability against polar solvent (ethanol). More importantly, the formation of $CsPbBr_3/SiO_2$ nanocomposites was achieved in the environmental solvent of mixed ethanol and water system, which may be reported for the first time and offer a green technique for perovskite composited with other barrier materials.

Materials and methods

Materials

Cesium bromide (CsBr, 99.5%), lead bromide ($PbBr_2$, 99.0%), oleylamine (OAm, 80–90%) and oleic acid (OA, 90%) were purchased from Aladdin. *N,N*-dimethylformamide (DMF, 99.9%), tetraethyl

orthosilicate (TEOS, 99%) and ethanol were purchased from Kelong. Ultrapure water was made in our laboratory by Smart-S15. All the chemicals in this work were used without further purification.

Synthesis of $CsPbBr_3$ nanoparticles

To synthesize green emissive $CsPbBr_3$ nanoparticles, CsBr (1.2 mmol) and $PbBr_2$ (0.4 mmol) were dissolved in DMF (10 mL) at room temperature. OAm (0.5 mL) and OA (1.0 mL) were added to the former solution. The precursor solution was stirred for a few hours until a feeble green emission was observed; the products were pasted on the inwall of the container. Then, residual transparent solution of precursor was discarded and the green luminescent products were retained. Subsequently, ethanol (14.8 mL) and ultrapure water (2 mL) were added in sequence, and a strong green emission was observed immediately. The solution was centrifuged at 8000 rpm, and the precipitate was collected for further characterization.

Synthesis of $CsPbBr_3/SiO_2$ composites

Similar to the synthesis of $CsPbBr_3$ nanoparticles, except for ethanol and ultrapure water, we also added TEOS (0 mL, 0.06 mL, 0.6 mL, 1.2 mL, 2.4 mL) as the precursor for silica. After vigorous stirring at room temperature for a few hours, a yellowish solution was formed and $CsPbBr_3/SiO_2$ composites were prepared in situ successfully.

Characterization

The scanning electron microscope (SEM) images were taken using FEI QUANTA FEG 250. X-ray diffraction (XRD) patterns of $CsPbBr_3$ and $CsPbBr_3/SiO_2$ composites were acquired using a Bruker D8 Advance X diffractometer (Cu Kα: $\lambda = 1.5406$ Å). Fluorescence emission spectra of the samples were measured using Edinburgh FLS980. Steady-state absorption spectra were recorded on a Shimadzu UV-2600 spectrophotometer.

Results and discussion

Typically, perovskite nanoparticles were synthesized by a traditional ligand-assisted reprecipitation method; the precursors of perovskites are usually dissolved in DMF and a supersaturated crystallization process will be completed in toluene sequentially [31, 32]. As suitable capping ligands, OA and OAm assist to control the phase structure and particle size collectively. Considering the instability of perovskite and toxicity stemmed from toluene solvent, we designed a reasonable experiment to shy away this weakness.

In our work, SiO_2 barrier material is exerted to improve chemical stability. Figure 1 shows the formation process of $CsPbBr_3/SiO_2$ composite particles. First, precursor solutions were prepared in DMF with different molar ratios of CsBr to $PbBr_2$ (5:1, 3:1, 1:1, 1:3 and 1:5). After CsBr and $PbBr_2$ were stirred in DMF for a few hours, it can be clearly seen that when the precursor ratios of the system were 5:1 and 3:1, the solutions were suspension liquid, and the others with decreased ratios were transparent. When CsBr was excessive, the low solubility of the coordination compound in DMF contributed to the suspension solution. Then, OA and OAm as ligands were added to the precursor solution and further promoted the formation of products on the inwall. An interesting phenomenon is observed that two samples displayed distinct green emission under 365 nm UV lamp irradiation and the corresponding photographs of these samples are shown in the inset of Fig. 2b. When the ratios of CsBr to $PbBr_2$ are 5:1 and 3:1, a light green emission can be observed, other three samples do not have the same characteristic. Due to the presence of OA and OAm, the fluorescent products adhere to the inner wall of the container and the remaining solution is transparent. When the transparent solution in DMF was substituted by ethanol, no quenching occurred on the light green emission product. X-ray diffraction (XRD) patterns and the photoluminescence (PL) spectrum were used to identify the emission product in Fig. 2. The PL spectrum of the typical sample with 3:1 ratio is shown in Fig. 2b, and the emission peak was located at 510 nm. Figure 2a shows the XRD patterns of the final product prepared with different ratios of CsBr to $PbBr_2$, which can determine the phase component of the products on the inwall of the container. When the molar ratios of CsBr to $PbBr_2$ ratio were 5:1 and 3:1, the XRD patterns demonstrated that Cs_4PbBr_6 particles were obtained with decreased amount of CsBr and excessive CsBr content maybe accelerates the formation of Cs_4PbBr_6. Since the luminescence property of Cs_4PbBr_6 is controversial, it is impossible

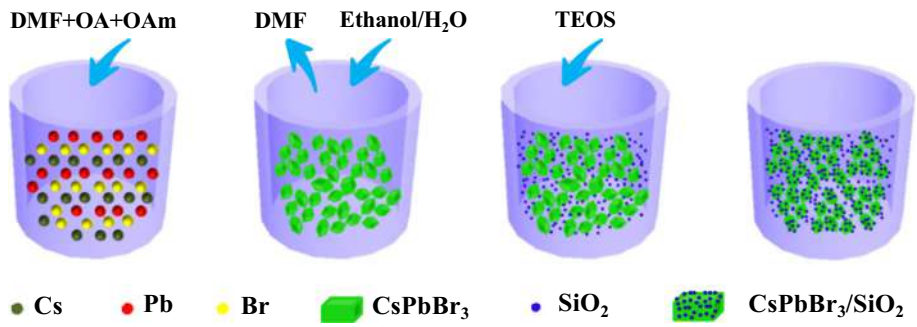

Figure 1 Schematic illustration of the formation process of $CsPbBr_3/SiO_2$ composite particles.

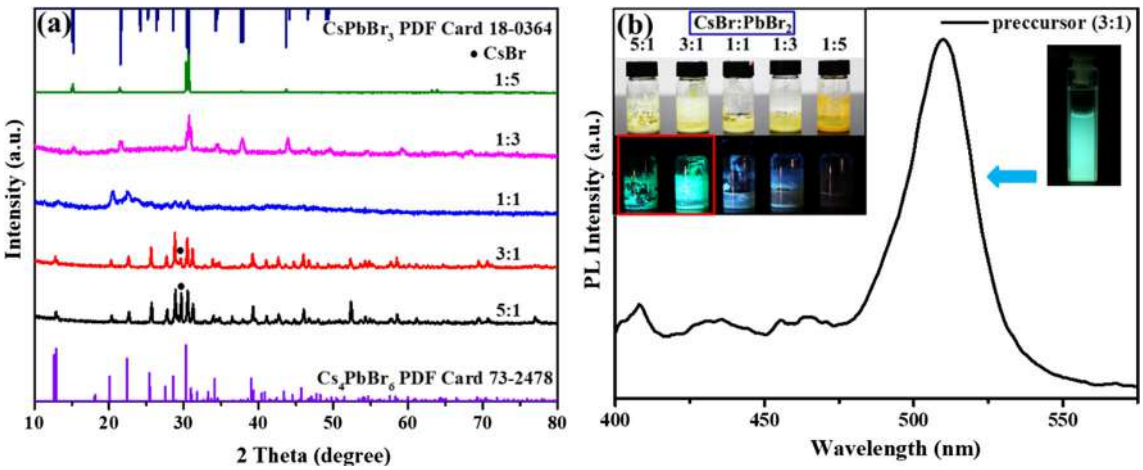

Figure 2 **a** XRD patterns of the products synthesized with different ratios of CsBr to $PbBr_2$ (5:1, 3:1, 1:1, 1:3 and 1:5). **b** PL spectrum of the sample synthesized with 3:1 ratio of CsBr to $PbBr_2$. The inset is photographs of perovskites precursors prepared with different ratios of CsBr to $PbBr_2$ under ambient light and 365 nm UV lamp irradiation.

to determine whether a little amount of $CsPbBr_3$ exists in the product according to XRD patterns. After decreasing the ratio to 1:3 and 1:5, $CsPbBr_3$ nanoparticles were the final product, but excessive $PbBr_2$ maybe causes fluorescence quenching of $CsPbBr_3$. Based on this outstanding peculiarity, the luminescent products on the inwall and an ethanol–water system were designed to prepare $CsPbBr_3/SiO_2$ composite to improve the stability of $CsPbBr_3$ nanoparticles. In this method, OAm as a Lewis base is used as both coating agent for $CsPbBr_3$ and one precursor for the formation of SiO_2, and in this way small SiO_2 particles were obtained by traditional Stöber method. After TEOS was added to the ethanol–water system, small SiO_2 nanoparticles attached to the surface of $CsPbBr_3$ nanoparticles and bright green emissive $CsPbBr_3/SiO_2$ nanocomposites were obtained.

When the ratio of CsBr to $PbBr_2$ was fixed at 3:1 and the amount of TEOS was 0.6 mL, the typical $CsPbBr_3/SiO_2$ nanocomposites were obtained. In this section, the morphology, structure and optical properties of the typical composites are investigated in detail and are shown in Fig. 3. To verify the formation mechanism, we carried out the experiments with and without TEOS and the products were characterized by SEM. As shown in Fig. 3a, monoclinic $CsPbBr_3$ nanoparticles were obtained, the size of small particles is around 200 nm, and a few big ones are around 1 um. After the addition of TEOS, SEM image shows two different morphologies of $CsPbBr_3/SiO_2$ nanocomposites in Fig. 3b. The small spherical particles of SiO_2 are around 20 nm, and the bigger monoclinic $CsPbBr_3$ nanoparticles are attached or encapsulated by SiO_2 matrix. The XRD spectrum without SiO_2 exhibits diffraction peaks at 15.1°, 21.5°, 30.6°, 37.5° and 43.7°, corresponding to (001), (110), (200), (121) and (202) planes, which indicates the monoclinic crystalline phase (Fig. 3c). Unlike bare $CsPbBr_3$ nanoparticles, a broad peak around 20° can be indexed to amorphous SiO_2 (JCPDS Card No: 01-082-1554), which is similar to other silica-coated

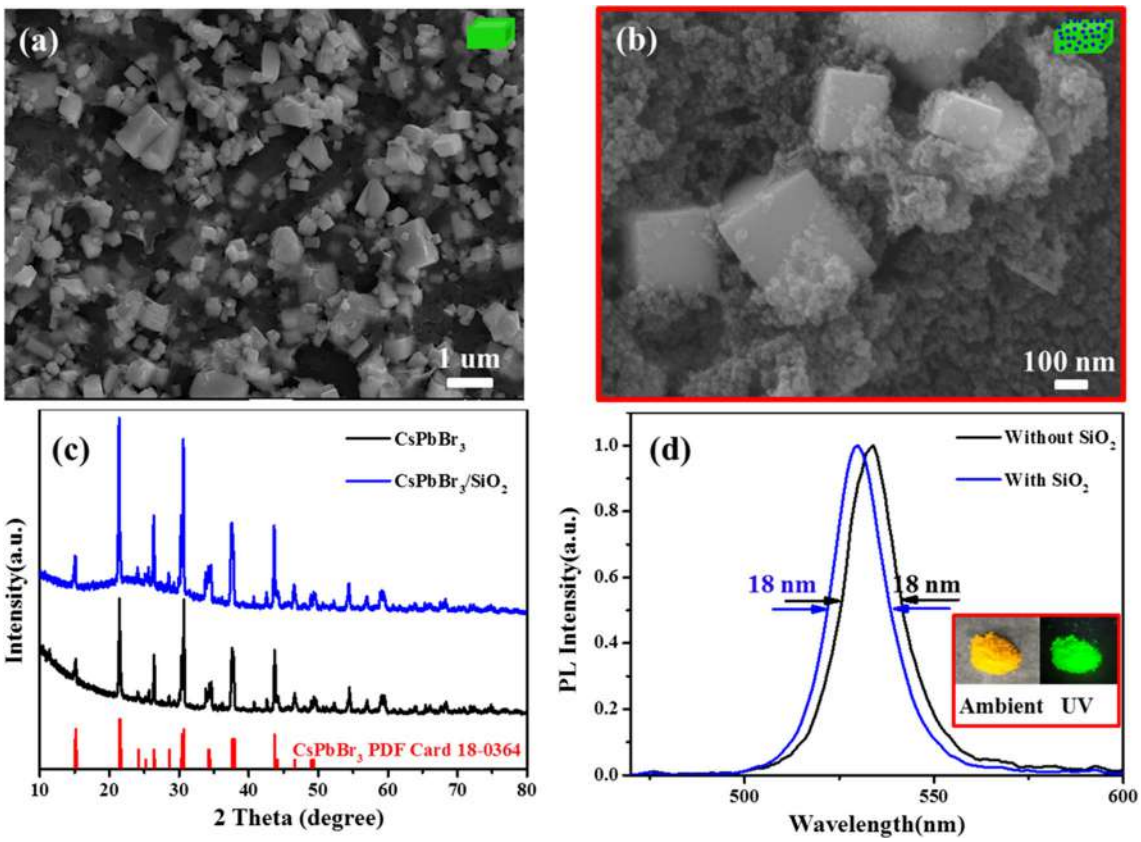

Figure 3 SEM images of **a** $CsPbBr_3$ nanoparticles and **b** $CsPbBr_3/SiO_2$ composite. **c** XRD patterns and **d** PL spectra of $CsPbBr_3$ and $CsPbBr_3/SiO_2$ nanoparticles. Insert shows the photographs of green $CsPbBr_3/SiO_2$ powders under ambient light and 365 nm UV lamp irradiation.

nanomaterials [28, 33]. The inserts in Fig. 3d show the photographs of green $CsPbBr_3/SiO_2$ powders under ambient light and 365 nm UV lamp irradiation, and the $CsPbBr_3/SiO_2$ powders reveal a bright green emission. The optical properties of the $CsPbBr_3$ nanoparticles with and without SiO_2 were studied by monitoring the PL of the nanocomposites in ethanol. The PL of $CsPbBr_3$ nanoparticles peaked at around 533 nm and $CsPbBr_3/SiO_2$ nanocomposites at around 529 nm, and the emission spectra all showed narrowed full-width half-maximum (18 nm). The successful synthesis of $CsPbBr_3/SiO_2$ nanocomposites in ethanol–water system makes a new door for improving the stability of perovskites in an environment method.

In addition, the amount of TEOS was investigated which was highly effected on the optical property of $CsPbBr_3/SiO_2$ nanocomposites. Due to strong scattering effects of SiO_2 materials, the distance between perovskite nanoparticles will be separated by abundant SiO_2 nanoparticles, which can inhibit the deterioration from polar solvent effectively. Figure 4a shows the photographs of $CsPbBr_3/SiO_2$ solutions prepared with different amount of TEOS (0 mL, 0.06 mL, 0.6 mL, 1.2 mL, 2.4 mL) under ambient light and 365 nm UV lamp irradiation. With the increase in TEOS amount, the yields in the container elevated. When the amount of TEOS is more than 0.6 mL, the increase in nanocomposites output is nonnegligible. As shown in Fig. 4b, $CsPbBr_3/SiO_2$ nanocomposites have higher PL intensity than bare $CsPbBr_3$ nanoparticles. Even a little content of TEOS (0.06 mL) can provide enough SiO_2 nanoparticles and the separation effect is also enough, owing to the small size of SiO_2 to separate perovskite nanoparticles forcefully. Compared to perovskite nanoparticles without the separation of SiO_2, there is remarkably an enhancement of larger than fivefold PL intensity with more TEOS (2.4 mL), evidently implying the great merit of SiO_2 spheres. The addition of SiO_2 nanoparticles barely influences the emission wavelength, the more SiO_2 nanoparticles, the perovskite nanoparticles more

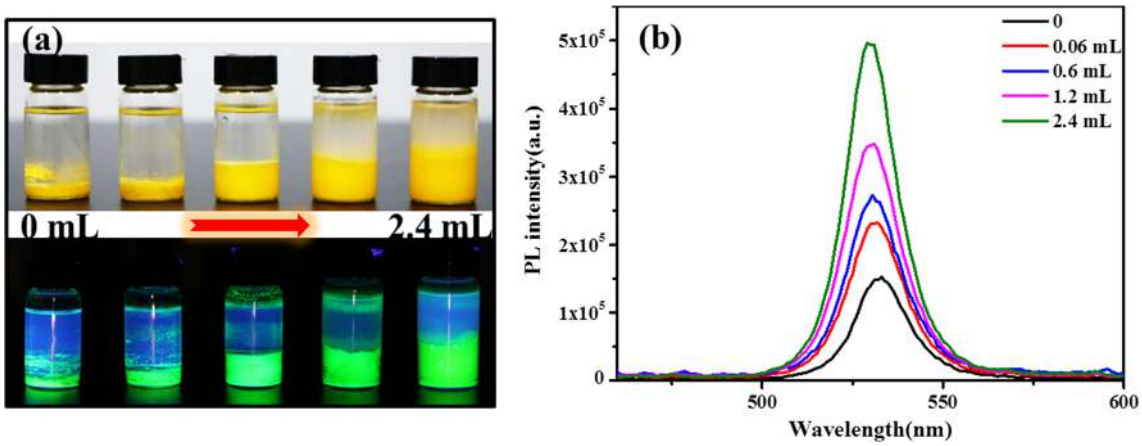

Figure 4 **a** Photographs of $CsPbBr_3/SiO_2$ samples prepared with different amount of TEOS (0 mL, 0.06 mL, 0.6 mL, 1.2 mL, 2.4 mL) under ambient light and 365 nm UV lamp irradiation. **b** PL spectra of the corresponding $CsPbBr_3/SiO_2$ samples.

dispersed and not easy to agglomerate, resulting in the blue shift of the peaks from 533 nm to 529 nm. Therefore, $CsPbBr_3/SiO_2$ nanocomposites with elevated photoluminescence have been synthesized using this simple and environmental method.

The stability of perovskites is highly relevant for its application in optoelectronic field, and here the variation of optical property in polar solvent was further studied. To evaluate the stability of $CsPbBr_3/SiO_2$ nanocomposites in ethanol, $CsPbBr_3$ nanoparticles without SiO_2 were also tested for comparison. The remnant PL intensities of the $CsPbBr_3$ nanoparticles without and with SiO_2 are displayed in Fig. 5c. As shown in Fig. 5a, the PL spectra of $CsPbBr_3$ nanoparticles have the highest intensity when the nanoparticles were dispersed in ethanol first time. It is well known that the $CsPbBr_3$ quantum dots prepared by hot injection method quickly quenched within several minutes after adding ethanol. But the $CsPbBr_3$ nanoparticles prepared by ethanol–water-assisted room temperature method experienced a PL quenching to 65% of initial PL intensity after immersing 24 h in ethanol. It is encouraging that $CsPbBr_3/SiO_2$ nanocomposites exhibit a PL enhancement when nanocomposites were immersed in ethanol for 96 h, which indicated that $CsPbBr_3$ without SiO_2 decomposed faster in polar solvent. Until to 168 h, the emission intensities of $CsPbBr_3$ nanoparticles and $CsPbBr_3/SiO_2$ nanocomposites were maintained at approximately 52% and 71% of the initial intensity, respectively. This result also can be confirmed from the insets of Fig. 5c; $CsPbBr_3$ nanoparticles dispersed in ethanol with SiO_2 showed brighter fluorescence than the unprotected ones. In brief, $CsPbBr_3$ nanoparticles decorated with small SiO_2 have enhanced stability against ethanol reliably.

XRD patterns and absorption spectra were used to investigate the evolution process of the samples under different experimental conditions. In Fig. 6a, the Cs_4PbBr_6 particles were converted into $CsPbBr_3$ after adding water and TEOS, mainly due to the deprivation of CsBr component out from the Cs_4PbBr_6 crystal triggered by H_2O molecules. After time degradation test, owing to the stripping of more CsBr in polar solvent, the intensities of the diffraction peaks of $CsPbBr_3$ gradually decreased, the less $CsPb_2Br_5$ and more $PbBr_2$ diffraction peaks emerged, and the $CsPbBr_3$ was degraded to $PbBr_2$ finally. The absorption spectra of these three samples are shown in Fig. 6b. The absorption spectra of the pristine material synthesized with OA and OAm and $CsPbBr_3/SiO_2$ composite are dominated by exciton peaks, which are approximately 528 nm belonged to $CsPbBr_3$. Maybe the Cs_4PbBr_6 products were formed with a few $CsPbBr_3$ particles. The corresponding degraded products also do not have this characteristic absorption peak. The absorption peak located at 305 nm can be assigned to $CsPb_2Br_5$ [34]. The above results further proved that the polar solvent can transform the perovskite phase structure by extracting CsBr from crystal lattice and lead to complete decomposition.

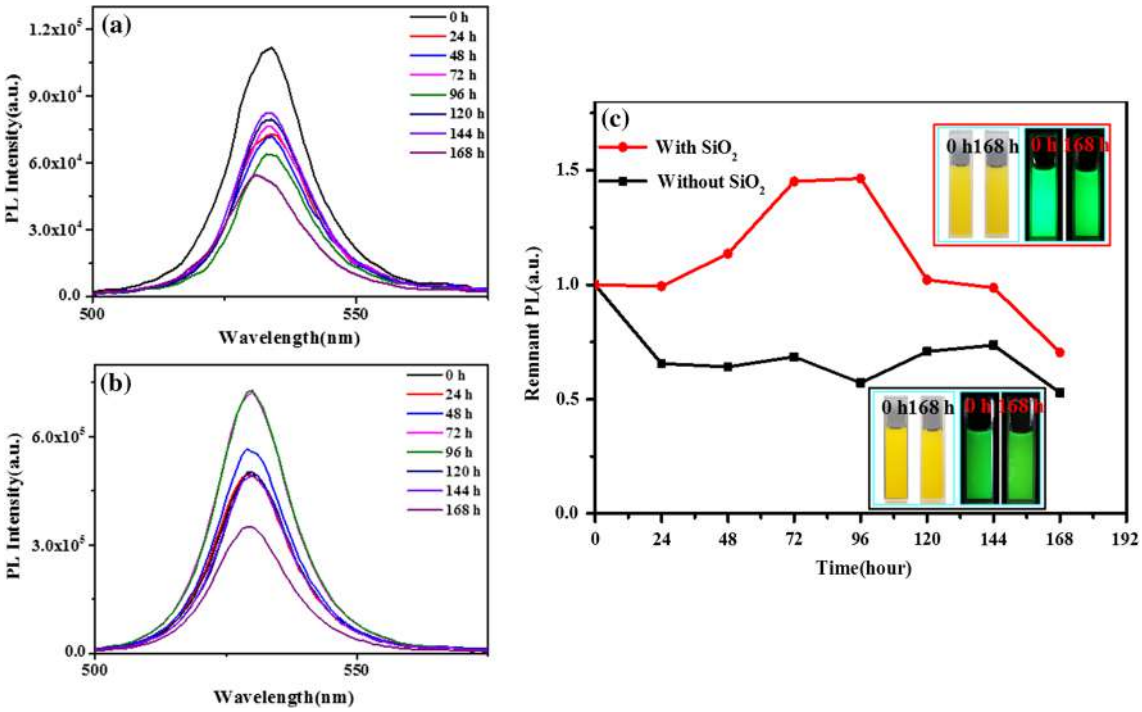

Figure 5 PL spectra of **a** $CsPbBr_3$ nanoparticles and **b** $CsPbBr_3/SiO_2$ nanocomposites dispersed in ethanol at different times (0–168 h). **c** Stability of $CsPbBr_3$ nanoparticles and $CsPbBr_3/SiO_2$ composite particles after dispersed in ethanol. Insets show the photographs of two samples before and after degradation in ethanol.

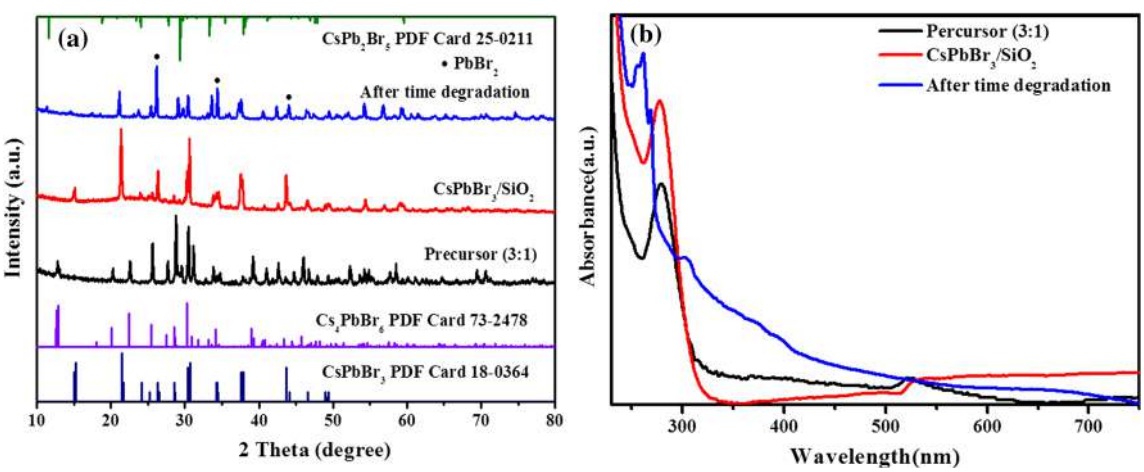

Figure 6 **a** XRD patterns and **b** absorption spectra of the pristine material synthesized with OA and OAm, $CsPbBr_3/SiO_2$ composite and the composite after the time degradation test.

Conclusion

In conclusion, $CsPbBr_3/SiO_2$ nanocomposites were synthesized using a one-pot and facile ethanol–water-assisted room temperature synthesis. The ethanol–water system is not only green and environmental but also conducive to the phase transformation and the formation of SiO_2 nanoparticles. The obtained $CsPbBr_3/SiO_2$ nanocomposites with high luminesce and narrow line width will be applied in high-quality lighting and display. $CsPbBr_3/SiO_2$ nanocomposites exhibit significantly improved environmental stability compared to the naked $CsPbBr_3$ nanoparticles dispersed in polar solvent. Our work provides a simple and environmentally synthetic strategy for highly luminescent nanocrystals; this

work will also open the window for new barrier materials synthesized in ethanol and water system to keep perovskite stable for longer time.

Acknowledgements

This work is supported by the Scientific and Technological Projects for International Cooperation Funds of Sichuan Science and Technology Program (Nos. 2017HH0069 and 2018RZ0074), the Fundamental Research Funds for the Central Universities of China (A0920502051408-10 and ZYGX2009Z0001) and Cultivation Program for the Excellent Doctoral Dissertation of Southwest Jiaotong University (No. D-YB201709).

Compliance with ethical standards

Conflict of interest The authors declare that they have no conflict of interest.

References

[1] Shi D, Adinolfi V, Comin R, Yuan MJ, Alarousu E, Buin A, Chen Y, Hoogland S, Rothenberger A, Katsiev K, Losovyj Y, Zhang X, Dowben PA, Mohammed OF, Sargent EH, Bakr OM (2015) Low trap-state density and long carrier diffusion in organolead trihalide perovskite single crystals. Science 347:519–522

[2] Ravi VK, Markad GB, Nag A (2016) Band edge energies and excitonic transition probabilities of colloidal $CsPbX_3$ (X = Cl, Br, I) perovskite nanocrystals. ACS Energy Lett 1:665–671

[3] Sun HZ, Yang ZY, Wei MY, Sun W, Li XY, Ye SY, Zhao YB, Tan HR, Kynaston EL, Schon TB, Yan H, Lu Z-H, Ozin GA, Sargent EH, Seferos DS (2017) Chemically addressable perovskite nanocrystals for light-emitting applications. Adv Mater 29:1701153

[4] Chu Q-Q, Ding B, Li Y, Gao L, Qiu Q, Li C-X, Li C-J, Yang G-J, Fang BZ (2017) Fast drying boosted performance improvement of low-temperature paintable carbon-based perovskite solar cell. ACS Sustain Chem Eng 5:9758–9765

[5] Li Z, Klein TR, Kim DH, Yang MJ, Berry JJ, van Hest MFAM, Zhu K (2018) Scalable fabrication of perovskite solar cells. Nat Rev Mater 3:18017

[6] Xiao ZG, Kerner RA, Zhao LF, Tran NL, Lee KM, Koh T-W, Scholes GD, Rand BP (2017) Efficient perovskite light-emitting diodes featuring nanometre-sized crystallites. Nat Photonics 11:108–115

[7] Abdi-Jalebi M, Andaji-Garmaroudi Z, Cacovich S, Stavrakas C, Philippe B, Richter JM, Alsari M, Booker EP, Hutter EM, Pearson AJ, Lilliu S, Savenije TJ, Rensmo H, Divitini G, Ducati C, Friend RH, Stranks SD (2018) Maximizing and stabilizing luminescence from halide perovskites with potassium passivation. Nature 555:497–501

[8] Li XM, Yu DJ, Chen J, Wang Y, Cao F, Wei Y, Wu Y, Wang L, Zhu Y, Sun ZG, Ji JP, Shen YL, Sun HD, Zeng HB (2017) Constructing fast carrier tracks into flexible perovskite photodetectors to greatly improve responsivity. ACS Nano 11:2015–2023

[9] Dou L, Yang YM, You J, Hong Z, Chang WH, Li G, Yang Y (2014) Solution-processed hybrid perovskite photodetectors with high detectivity. Nat Commun 5:5404

[10] Veldhuis SA, Boix PP, Yantara N, Li MJ, Sum TC, Mathews N, Mhaisalkar SG (2016) Perovskite materials for light-emitting diodes and lasers. Adv Mater 28:6804–6834

[11] Sun WZ, Wang KY, Gu ZY, Xiao SM, Song QH (2016) Tunable perovskite microdisk lasers. Nanoscale 8:8717–8721

[12] Weidman MC, Goodman AJ, Tisdale WA (2017) Colloidal halide perovskite nanoplatelets: an exciting new class of semiconductor nanomaterials. Chem Mater 29:5019–5030

[13] Shi ZF, Li S, Li Y, Ji HF, Li XJ, Wu D, Xu TT, Chen YS, Tian YT, Zhang YT, Shan CX, Du GT (2018) Strategy of solution-processed all-inorganic heterostructure for humidity/temperature-stable perovskite quantum dot light-emitting diodes. ACS Nano 12:1462–1472

[14] Akkerman QA, RainòG Kovalenko MV, Manna L (2018) Genesis, challenges and opportunities for colloidal lead halide perovskite nanocrystals. Nat Mater 15:394–405

[15] Liu F, Zhang YH, Ding C, Kobayashi S, Izuishi T, Nakazawa N, Toyoda T, Ohta T, Hayase S, Minemoto T, Yoshino K, Dai SY, Shen Q (2017) Highly luminescent phase-stable $CsPbI_3$ perovskite quantum dots achieving near 100% absolute photoluminescence quantum yield. ACS Nano 11:10373–10383

[16] Krieg F, Ochsenbein ST, Yakunin S, Brinck ST, Aellen P, Süess A, Clerc B, Guggisberg D, Nazarenko O, Shynkarenko Y, Kumar S, Shih C-J, Infante I, Kovalenko MV (2018) Colloidal $CsPbX_3$ (X = Cl, Br, I) nanocrystals 2.0: zwitterionic capping ligands for improved durability and stability. ACS Energy Lett 3:641–646

[17] Pan J, Shang YQ, Yin J, Bastiani MD, Peng W, Dursun I, Sinatra L, El-Zohry AM, Hedhili MN, Emwas A-H, Mohammed OF, Ning ZJ, Bakr OM (2018) Bidentate ligand-passivated $CsPbI_3$ perovskite nanocrystals for stable near-unity photoluminescence quantum yield and efficient red light-emitting diodes. J Am Chem Soc 140:562–565

[18] Xin YM, Zhao HJ, Zhang JY (2018) Highly stable and luminescent perovskite – polymer composites from a convenient and universal strategy. ACS Appl Mater Interfaces 10:4971–4980

[19] Hou SC, Guo YZ, Tang YG, Quan QM (2017) Synthesis and stabilization of colloidal perovskite nanocrystals by multidentate polymer micelles. ACS Appl Mater Interfaces 9:18417–18422

[20] Yoon HC, Lee S, Song JK, Yang H, Do YR (2018) Efficient and stable CsPbBr 3 quantum-dot powders passivated and encapsulated with a mixed silicon nitride and silicon oxide inorganic polymer matrix. ACS Appl Mater Interfaces 10:11756–11767

[21] Li Z-J, Hofman E, Li J, Davis AH, Tung C-H, Wu L-Z, Zheng WW (2018) Photoelectrochemically active and environmentally stable CsPbBr 3/TiO2 core/shell nanocrystals. Adv Funct Mater 28:1704288

[22] Loiudice A, Saris S, Oveisi E, Alexander DTL, Buonsanti R (2017) CsPbBr 3 QD/AlOx inorganic nanocomposites with exceptional stability in water, light, and heat. Angew Chem Int Ed 56:10696–10701

[23] Vassilakopoulou A, Papadatos D, Koutselas I (2016) Light emitting diodes based on blends of quasi-2D lead halide perovskites stabilized within mesoporous silica matrix. Micropor Mesopor Mater 249:165–175

[24] Vassilakopoulou A, Papadatos D, Koutselas I (2017) Flexible, cathodoluminescent and free standing mesoporous silica films with entrapped quasi-2D perovskites. Appl Surf Sci 400:434–439

[25] Dirin D, Protesescu L, Trummer D, Kochetygov IV, Yakunin S, Krumeich F, Stadie NP, Kovalenko MV (2016) Harnessing defect-tolerance at the nanoscale: highly luminescent lead halide perovskite nanocrystals in mesoporous silica matrixes. Nano Lett 16:5866–5874

[26] Malgras V, Tominaka S, Ryan JW, Henzie J, Takei T, Ohara K, Yamauchi Y (2016) Observation of quantum confinement in monodisperse methylammonium lead halide perovskite nanocrystals embedded in mesoporous silica. J Am Chem Soc 138:13874–13881

[27] Wang H-C, Lin S-Y, Tang A-C, Singh BP, Tong H-C, Chen C-Y, Lee Y-C, Tsai T-L, Liu R-S (2016) Mesoporous silica particles integrated with all-inorganic CsPbBr 3 perovskite quantum-dot nanocomposites (MP-PQDs) with high stability and wide color gamut used for backlight display. Angew Chem Int Ed 55:7924–7929

[28] Sun C, Zhang Y, Ruan C, Yin CY, Wang XY, Wang YD, Yu WW (2016) Efficient and stable white LEDs with silica-coated inorganic perovskite quantum dots. Adv Mater 28:10088–10094

[29] Li XM, Wang Y, Sun HD, Zeng HB (2017) Amino-mediated anchoring perovskite quantum dots for stable and low-threshold random lasing. Adv Mater 29:1701185

[30] Hu HC, Wu LZ, Tan YS, Zhong QX, Chen M, Qiu YH, Yang D, Sun BQ, Zhang Q, Yin YD (2018) Interfacial synthesis of highly stable $CsPbX_3$/oxide janus nanoparticles. J Am Chem Soc 140:406–412

[31] Li XM, Wu Y, Zhang SL, Cai B, Gu Y, Song JZ, Zeng HB (2016) $CsPbX_3$ quantum dots for lighting and displays: room-temperature synthesis, photoluminescence superiorities, underlying origins and white light-emitting diodes. Adv Funct Mater 26:2584

[32] Zhang F, Zhong HZ, Chen C, Wu X-G, Hu XM, Huang HL, Han JB, Zou BS, Dong YP (2015) Brightly luminescent and color-tunable colloidal $CH_3NH_3PbX_3$ (X = Br, I, Cl) quantum dots: potential alternatives for display technology. ACS Nano 9:4533–4542

[33] Chen Y, Yu MH, Ye S, Song J, Qu JL (2018) All-inorganic CsPbBr 3 perovskite quantum dots embedded in dual-mesoporous silica with moisture resistance for two-photon-pumped plasmonic nanolasers. Nanoscale 10:6704–6711

[34] Yang HZ, Zhang YH, Pan J, Yin J, Bakr OM, Mohammed OF (2017) Room-temperature engineering of all-inorganic perovskite nanocrystals with different dimensionalities. Chem Mater 29:8978–8982